



## Inhibitive effect of *Carica papaya* seed extract on aluminium in H<sub>2</sub>SO<sub>4</sub> medium

Pushpanjali M, Suma A Rao, Padmalatha Rao\*

Department of Chemistry, Manipal Institute of Technology, Manipal University, Karnataka, 576104, India

Received 14 Oct 2013, Revised 15 Oct 2013, Accepted 15 Oct 2013

\*Corresponding Author [padmalatha.rao@manipal.edu](mailto:padmalatha.rao@manipal.edu).

### Abstract

The inhibitive effect Carica papaya seed extract (CPSE) on the corrosion behavior of aluminium in sulphuric acid medium of pH 2.3 was investigated by using Tafel polarization and electrochemical impedance spectroscopy (EIS) techniques in the temperature range 30 to 50°C. The concentration of inhibitors used was in the range of 100-400ppm. The surface morphology was studied using scanning electron microscopy (SEM). Inhibition efficiency was found to increase with increase in inhibitor concentration and decrease with increase in temperature. CPSE acted as a mixed type inhibitor. Inhibitor underwent physisorption on the surface of the metal and followed Langmuir adsorption isotherm. The kinetic and thermodynamic parameters were calculated and discussed in detail.. CPSE emerged as a potential, cost effective eco-friendly natural inhibitor for the corrosion control of aluminium in sulphuric acid medium.

**Keywords:** Aluminium , Green inhibitor, Carica papaya, Tafel polarisation, EIS studies, SEM

### 1. Introduction

Corrosion control studies of aluminium and aluminium alloys are of prime importance for researchers because of their technological and economic considerations. Aluminium and aluminium alloys find immense applications in automobiles, aviation, household appliances, containers and electronic devices [1-3]. The applications of aluminium and its alloys are often possible because of the natural tendency of aluminium to form a passivating oxide layer. However in aggressive media, the passivating layer can be destroyed and corrosive attack can take place. The protection of aluminium and its oxide films against the corrosive action of chloride and sulphate ions have been extensively studied [4-5]. Hydrochloric and sulphuric acid in the pH range of 2-4.5 is mainly used for pickling of aluminium and its alloys [6]. A useful method to protect metals and alloys deployed in service in aggressive environments against corrosion is the addition of inhibitors. A number of organic compounds are known to be applicable as corrosion inhibitors for aluminium and its alloys in acidic environments [7-9]. However, increased awareness of environmental hazards caused by synthetic chemicals has received global attention. There exists a need to develop a new class of corrosion inhibitors with low toxicity and good efficiency. The exploration of natural products of plant origin as inexpensive eco-friendly inhibitor is an essential field study [10-12]. Till date lots of works have been reported for using natural product as corrosion inhibitors [13-15] including barks and leaves of carica papaya for aluminium and steel in acidic media. As a part of our research work with natural inhibitors for the corrosion control of aluminium and its alloys [16-18], we report herein, the results of utility of Carica papaya seed extract (CPSE) for the corrosion control of aluminium in sulphuric acid medium of pH 2.3. This study has dual purposes, first to study the corrosion behavior of aluminium at lowest possible concentration of sulphuric acid medium and secondly to establish the effectiveness of extract CPSE as corrosion inhibitor.

### 2. Materials and methods

#### 2.1. Material

The composition of aluminium is: Si: 0.467%, Fe: 0.163%, Mg: 0.530% and aluminium: Balance. Cylindrical test coupons of 10 mm diameter and approximately 20 mm height were machined from the rods of aluminium and metallographically mounted up to 10mm height using cold setting resin. The exposed flat surface of the mounted part was polished as per standard metallographic practice - belt grinding followed by polishing on emery papers and finally disc polished using levigated alumina abrasive.

#### 2.2. Medium

Sulphuric acid solution of required strength was prepared from previously standardised stock solution of 2M solution.

#### 2.3. Preparation and characterization of seeds of Carica papaya extract (CPSE)

The aqueous extract of the CPSE was prepared by literature method [21]. 40 g of the powdered Carica papaya seeds were boiled in 500 ml of distilled water for 30 minutes after which it was filtered using a piece of clean white cotton gauze. The filtrate was evaporated to complete dryness at 40°C, producing a fine sweet smelling and chocolate colour solid residue. The solid residue obtained was weighed and pooled together in an air and water-proof container kept in a refrigerator at 4°C.

FTIR of the solid residue was recorded using spectrophotometer (Shimmed model) in the frequency range of 4000 to 400cm<sup>-1</sup> using Kerr pellet. Aqueous solution of required strengths was prepared whenever required.

#### 2.4. Electrochemical measurements.

The Teal polarization studies were carried out by using a potentiostat (CH 600D series US Model with CH instrument beta software) and a three electrode cell. The electrochemical cell used was a conventional three Pyrex glass cell with a platinum counter electrode and a saturated calomel electrode (SCE) as reference electrode. The working electrode was made up of aluminium sample. Polished aluminium specimen with 0.95cm<sup>2</sup> surface area was exposed to 50mL of sulphuric acid (pH=2.3) at 30°C without and with 100, 200, 300 and 400ppm inhibitors in the acid solution. The steady state open circuit potentials with respect to SCE were noted at the end of 5 minutes. The polarization studies were then made from -250mV to +250mV Vs respective OCP with a scan rate of 1mV sec<sup>-1</sup> and corresponding corrosion currents recorded. From Tafel plots various potentiodynamic parameters were determined. The corrosion rate in mmy<sup>-1</sup> was calculated using equation (1).

$$v_{corr} (\text{mm y}^{-1}) = \frac{3270 \times M \times i_{corr}}{\rho \times Z} \quad (1)$$

where 3270 is a constant that defines the unit of corrosion rate,  $i_{corr}$  = corrosion current density in A cm<sup>-2</sup>,  $\rho$  = density of the corroding material,  $M$  = Atomic mass of the metal, and  $Z$  = Number of electrons transferred per metal atom [22].

The percentage inhibition efficiency was calculated from expression (2).

$$\eta(\%) = \frac{i_{corr} - i_{corr(inh)}}{i_{corr}} \times 100 \quad (2)$$

where  $i_{corr}$  and  $i_{corr(inh)}$  are the corrosion current densities in the absence and in the presence of inhibitor, respectively. The experiments were repeated for 35, 40, 45 and 50°C and  $E_{corr}$ ,  $i_{corr}$ , corrosion rate (CR) and % IE were determined.

The corrosion rates for all the above conditions are also obtained from electrochemical impedance measurement technique carried out in a frequency range from 0.01 to 10000Hz using a small amplitude ac signal of 10mV at the open circuit potential and resulting impedance data were analyzed using Nyquist plots. Charge transfer resistance ( $R_{ct}$ ) and double layer capacitance ( $C_{dl}$ ) were recorded.

The inhibition was calculated using equation (3):

$$\eta(\%) = \frac{RP(inh.) - RP}{RP(inh.)} \times 100 \quad (3)$$

where  $R_p^1$  and  $R_p$  are the polarization resistances in the presence and absence of inhibitors.

#### 2.5. Scanning electron microscopy

The surface morphology of aluminium surface, in absence and in the presence of the inhibitor was studied by immersing the material in sulphuric acid of pH 2.3 for 2 hrs. using JEOL JSM-6380L Analytical scanning electron microscope.

### 3. Results and discussion

#### 3.1 Fourier transform infrared (FTIR) spectroscopy of CPSE

Figure 1 shows the FTIR spectrum of CPE. -N=C=S Stretching frequency appears at 2300cm<sup>-1</sup>. The Aromatic Stretching frequency appears at 3050cm<sup>-1</sup>. The -C=C- Stretching frequency at 1612cm<sup>-1</sup>.

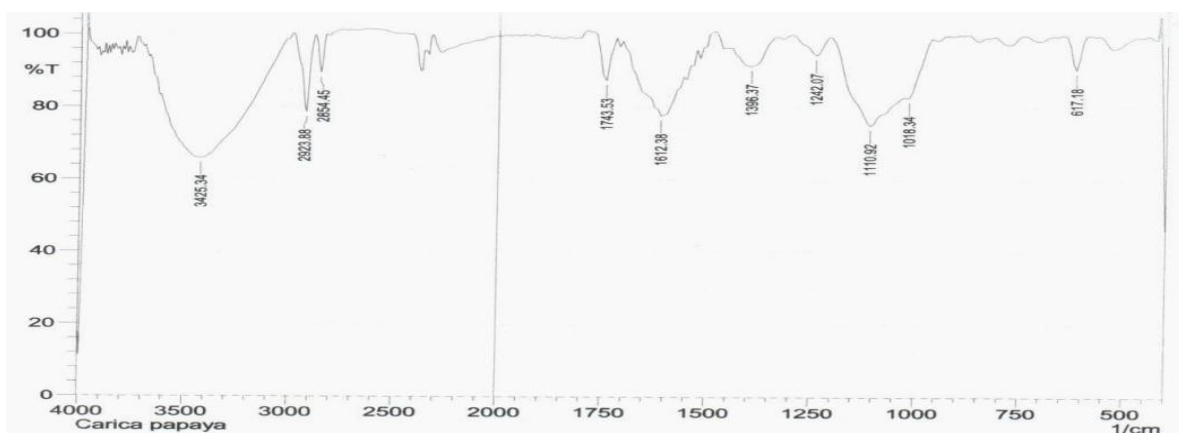


Figure 1: IR spectra of Carica papaya seed extract

#### 3.2. Potentiodynamic polarization curves

Figure 2 shows the Tafel polarization curves of aluminium in sulphuric acid of 2.3pH at 30 °C for different concentrations of inhibitor. Valuable potentiodynamic parameters such as corrosion current density ( $i_{corr}$ ), corrosion potential ( $E_{corr}$ ), anodic and cathodic slopes ( $b_a$  and  $b_c$ ) were obtained from Figure 2. Corrosion rate and % efficiency of the inhibitor was calculated using equation 1 and 2 respectively. Results are tabulated in Table 1.

From Table 1, is evident that corrosion current density ( $i_{\text{corr}}$ ) and corrosion rate decreased with increase in the concentration of inhibitor. Inhibition efficiency increased with increasing inhibitor concentrations. The parallel cathodic Tafel curves suggest that the hydrogen evolution is activation controlled, and the reduction mechanism is not affected by the presence of the inhibitors [23]. The values of  $-b_c$  changes with increase in inhibitor concentration which indicates the influence of seeds of *Carica papaya* on the kinetics of hydrogen evolution. The shift in the anodic Tafel slope  $b_a$  may be due to the sulfate/inhibitor molecules adsorbed on the aluminium surface.

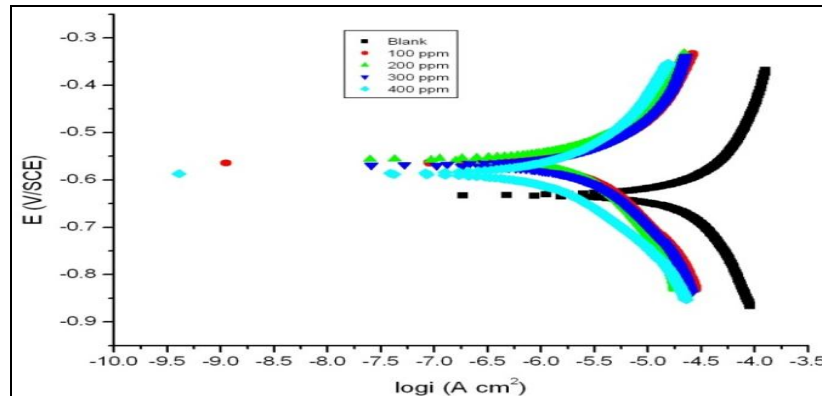


Figure 2: Tafel plot for aluminium in  $\text{H}_2\text{SO}_4$  (pH= 2.3) at 30 C for different concentrations CPSE.

No definite trend is observed in the variation of corrosion potential ( $E_{\text{corr}}$ ) values, which suggests that seeds of *Carica papaya* act as a mixed type inhibitor [23]. According to Ferreira et al and Li et al.[24, 25], if the displacement in corrosion potential is more than  $\pm 85$  mV with respect to corrosion potential of the blank, then the inhibitor can be considered as a cathodic or anodic type. However, the maximum displacement in this study is not more than 30 mV, which indicates that inhibitor is a mixed type inhibitor.

### 3.3. Electrochemical impedance spectroscopy (EIS) studies

In order to gain more information about the corrosion inhibition phenomenon, electrochemical impedance spectroscopy measurements were carried out for the aluminium in sulphuric acid of pH 2.3 in the presence and absence of aqueous extracts of seeds of *Carica papaya* at different temperatures.

Figure 3 represents Nyquist plot of aluminium in the presence of various concentrations of aqueous extracts of seeds of *Carica papaya* in a solution containing sulphuric acid of pH 2.3 at 30°C. Similar results were obtained at other temperatures studied. The impedance diagrams of Figure 3 show semicircles. This indicates that the corrosion process is mainly charge transfer controlled. The presence of inhibitor increases the impedance but does not change other aspects of the behaviour[25]. These results support the results of polarization measurements that the inhibitor does not alter the mechanism of electrochemical reactions responsible for corrosion. It inhibits corrosion primarily through its adsorption on the metal surface [26].

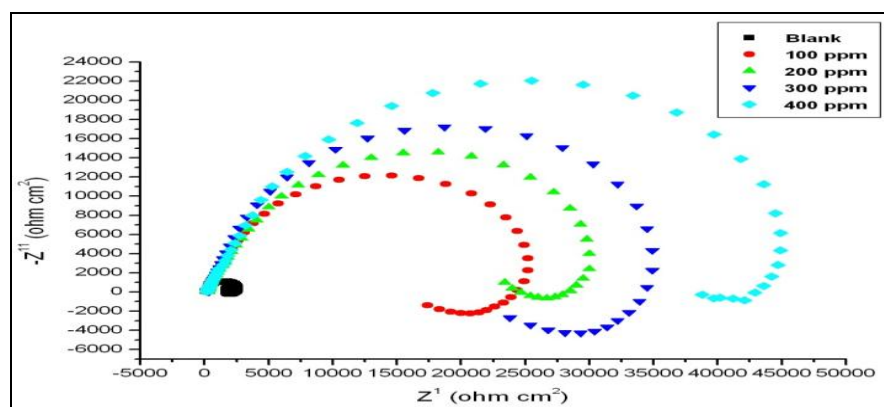


Figure 3: Nyquist plot for aluminium in  $\text{H}_2\text{SO}_4$  (pH= 2.3) at 35°C for different concentrations of CPSE

The impedance plots are with a depressed capacitive loop at high-frequency range (HF) whose diameter increases with increase in inhibitor concentration, followed by an inductive loop at low-frequency (LF) region. Similar impedance plots have been reported in the literature for the corrosion of pure aluminum and aluminum alloys in various electrolytes [27–28]. The high frequency capacitive loop could be assigned to the charge transfer of the corrosion process and to the formation of oxide layer [29]. The oxide film is considered to be a parallel circuit of a resistor due to the ionic conduction in the oxide film and a capacitor due to its dielectric properties. According to Brett [30], the capacitive loop is corresponding to the interfacial reactions, particularly, the reaction of aluminum oxidation at the metal/oxide/electrolyte interface.

**Table 1:** Results of Tafel polarization studies of aluminium in H<sub>2</sub>SO<sub>4</sub> ( pH=2.3) at different concentrations of CPSE

Temp (°C)	[CPSE] (ppm)	i <sub>Corr.</sub> (×10 <sup>-5</sup> ) (A/cm <sup>2</sup> )	C.R. (mmy <sup>-1</sup> )	ba (mV/dec <sup>1</sup> )	-bc (mV/dec <sup>1</sup> )	E <sub>corr.</sub> (mVvsSCE)	% η
30	0	3.83	0.45	414	282	-590	-----
	100	0.39	0.04	548	470	-560	89.87
	200	0.26	0.03	695	610	-610	94.60
	300	0.17	0.02	702	626	-640	95.49
	400	0.12	0.01	713	591	-610	96.78
35	0	4.13	0.44	394	363	-630	-----
	100	0.67	0.08	525	430	-530	83.75
	200	0.32	0.04	591	480	-560	92.30
	300	0.28	0.03	600	506	-570	93.34
	400	0.15	0.02	643	643	-590	96.40
40	0	5.19	0.57	335	375	-690	-----
	100	0.93	0.11	489	544	-610	82.00
	200	0.59	0.11	544	635	-590	88.70
	300	0.57	0.11	567	427	-640	89.06
	400	0.42	0.07	556	583	-610	91.80
45	0	5.76	0.60	369	579	-720	-----
	100	1.00	0.37	842	356	-610	81.69
	200	0.95	0.17	779	349	-620	82.60
	300	0.86	0.16	784	416	-670	84.30
	400	0.59	0.16	824	383	-640	89.27
50	0	5.48	0.66	321	421	-590	-----
	100	1.64	0.19	453	503	-560	71.49
	200	1.06	0.12	513	468	-610	81.56
	300	0.96	0.11	510	440	-640	83.27
	400	0.86	0.10	394	592	-610	85.11

The process includes the formation of Al<sup>+</sup> ions at the metal/oxide interface, and their migration through the oxide/solution interface where they are oxidized to Al<sup>3+</sup>. At the oxide/solution interface, OH<sup>-</sup> or O<sup>2-</sup> ions are also formed. The fact that all the three processes are represented by only one loop could be attributed either to the overlapping of the loops of processes, or to the assumption that one process dominates and, therefore, excludes the other processes [31]. The other explanation offered to the high frequency capacitive loop is the oxide film itself. This was supported by a linear relationship between the inverse of the capacitance and the potential found by Bessone et al. [32] and Wit and Lenderink [33]. The origin of the inductive loop has often been attributed to surface or bulk relaxation of species in the oxide layer [34]. The LF inductive loop may be related to the relaxation process obtained by adsorption and incorporation of sulphate ions, oxide ion and charged intermediates on and into the oxide film. The results are tabulated in Table 2.

As seen from Figure 3 that R<sub>s</sub> (solution resistance) remains almost constant, with and without addition of aqueous extracts of seeds of Carica papaya for aluminium. It was also observed that the value of constant phase element Q, decreases, while the values of R<sub>t</sub> increase with increasing concentration of inhibitor, indicating that the inhibition efficiency increases with the increase in concentration of aqueous extracts of seeds of Carica papaya. The double layer between the charged metal surface and the solution is considered as an electrical capacitor. The adsorption of inhibitor on the aluminum surface decreases its electrical capacity because they displace the water molecules and other ions originally adsorbed on the surface. The decrease in this capacity with increase in inhibitor concentrations may be attributed to the formation of a protective layer on the electrode surface. The thickness of this protective layer increases with increase in inhibitor concentration up to their critical concentration and then decreases. The obtained CPE (Q) values decrease noticeably with increase in the concentration of inhibitors.

An appropriate equivalent circuit is simulated for the observed impedance values. It is shown in Figure 4. In this equivalent circuit R<sub>s</sub> is the solution resistance and R<sub>t</sub> is the charge transfer resistance. R<sub>L</sub> and L represents the inductive elements. CPE (Q) is constant phase element in parallel to the series capacitors C<sub>1</sub>, C<sub>2</sub> and series resistors R<sub>1</sub>, R<sub>2</sub>, R<sub>L</sub> and R<sub>t</sub>. R<sub>L</sub> is parallel with the inductor L.

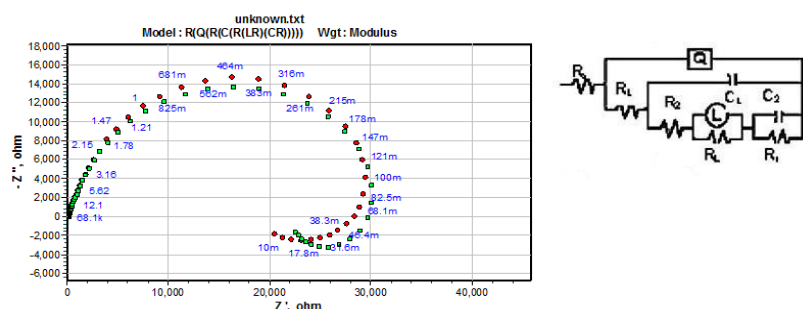


**Figure 4:** Equivalent circuit used to fit the experimental EIS data for the corrosion of aluminium in sulphuric acid of pH=2.3

**Table 2:** EIS data of aluminium in H<sub>2</sub>SO<sub>4</sub> (pH =2.3) in the presence of different concentrations of inhibitor CPSE

Temp. (°C)	[CPSE] (ppm)	C <sub>dl</sub> × 10 <sup>-10</sup> (F/cm <sup>2</sup> )	R <sub>ct</sub> (ohmcm <sup>2</sup> )	% η
30	0	144.5	3537.6	----
	100	3.2	19777.1	82.1
	200	2.1	26069.5	86.4
	300	1.1	33613.0	89.5
	400	0.8	36287.9	90.2
35	0	235.1	3061.2	----
	100	3.6	17604.4	86.6
	200	2.2	20520.0	85.0
	300	2.0	27362.0	88.0
	400	1.1	33007.1	90.0
40	0	316.7	2880.4	----
	100	6.5	15965.6	82.0
	200	5.2	17231.0	83.3
	300	3.1	20069.5	85.6
	400	2.7	26069.5	89.0
45	0	456.4	2384.6	----
	100	8.9	13234.8	81.0
	200	7.9	14225.3	83.0
	300	7.8	15429.7	84.5
	400	4.1	19877.1	87.9
50	0	993.6	1586.5	----
	100	46.7	6472.7	75.0
	200	22.1	7127.1	77.7
	300	15.4	10780.2	85.3
	400	9.1	11393.3	86.0

The double layer capacitance C<sub>dl</sub> can be calculated from equation (4)

$$C_{dl} = C_1 + C_2 \quad (4)$$

And the polarization resistance R<sub>p</sub> is calculated using the equation (5)

$$R_p = R_L + R_t + R_1 + R_2 \quad (5)$$

Since R<sub>p</sub> is inversely proportional to the corrosion current and it can be used to calculate the percentage inhibition efficiency using the relation (3).

### 3.4. Effect of temperature

From Table 1 it is evident that efficiency decreased with increasing temperature. This indicates desorption of inhibitor molecules [35]. However, at higher concentration of inhibitor this decrease is small. The study of effect of temperature was used to calculate energy of activation (E<sub>a</sub>) for the corrosion process in the presence and absence of inhibitor using Arrhenius law Equation (6) [36].

$$\ln(CR) = B - \left(\frac{E_a}{RT}\right) \quad (6)$$

where B is a constant which depends on the metal type and R is the universal gas constant, T is the absolute temperature. The Arrhenius plots for the commercial sample of aluminum are shown in Figure 5.

The plot of ln(CR) versus 1/T gives straight line whose slope = -E<sub>a</sub>/R gives activation energy for the corrosion process.

The enthalpy (ΔH<sub>a</sub>) and entropy of activation values (ΔS<sub>a</sub>) for the dissolution of specimen were calculated from transition state Equation (7) [36].

$$CR = RT \frac{RT}{Nh} \exp\left(\frac{\Delta S_a}{R}\right) \exp\left(-\frac{\Delta H_a}{RT}\right) \quad (7)$$

where h is Plank's constant and N is Avogadro's number.

A plot of ln (corrosion rate/T) versus 1/T gives straight line with slope = -ΔH<sub>a</sub>/R and intercept = ln(R/Nh) + ΔS<sub>a</sub>/R. The plot of ln (corrosion rate/T) versus 1/T for aluminium in various concentrations of inhibitor in sulphuric acid of pH 2.3 is shown in Figure 6. The calculated values of E<sub>a</sub>, ΔH<sub>a</sub> and ΔS<sub>a</sub> are given in Table 3.

**Table 3:** Activation parameters for the corrosion of aluminium in H<sub>2</sub>SO<sub>4</sub> (pH=2.3)

Conc. (ppm)	E <sub>a</sub> (kJ/mol)	R <sup>2</sup>	ΔH <sub>a</sub> (kJ/mol)	ΔS <sub>a</sub> (J/K/mol)
0	17.20	0.99	14.60	-203.80
100	78.01	0.99	75.41	-369.43
200	83.40	0.96	80.80	-390.81
300	88.87	0.98	86.26	-402.86
400	107.77	0.97	105.17	-460.67

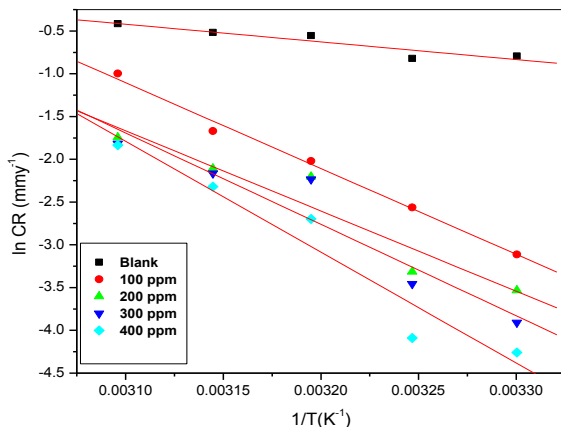


**Figure 5:** Plot of  $\ln(CR)$  Vs  $1/T$  for the corrosion inhibition of aluminium in  $H_2SO_4$  (pH =2.3)

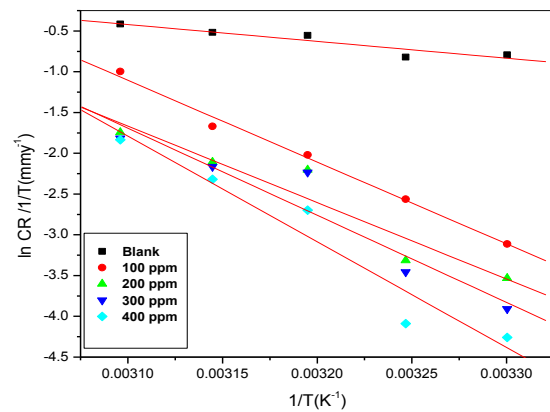


**Figure 6:** Plot of  $\ln(CR/T)$  Vs  $1/T$  for the corrosion inhibition of aluminium in  $H_2SO_4$  (pH =2.3)

The data in the tables show that the values of  $E_a$  of the corrosion of aluminium in the acid medium in the presence of aqueous extracts of seeds of *Carica papaya* are higher than those in the uninhibited medium. The increase in the activation energies with increasing concentration of the inhibitor is attributed to physical adsorption of inhibitor molecules on the metal surface. The adsorption of the inhibitor molecules on the surface of the aluminium blocks the charge transfer during corrosion reaction, thereby increasing the activation energy. In other words, the adsorption of the inhibitor on the electrode surface leads to the formation of a physical barrier that reduces the metal reactivity in the electrochemical reactions of corrosion [37]. The inhibition efficiency decreases with increase in temperature which indicates desorption of inhibitor molecule as the temperature increases [38]. The values of  $\Delta S_a$  are higher for inhibited solutions than those for the uninhibited solutions. This suggested that an increase in randomness occurred on going from reactants to the activated complex. This might be the results of the adsorption of organic compound present in the seeds of *Carica papaya* from the acidic solution which could be regarded as a quasi-substitution process between the organic compound in the aqueous phase and water molecules at electrode surface. In this situation, the adsorption of inhibitor is accompanied by desorption of water molecules from the surface. Thus the increase in entropy of activation was attributed to the increase in solvent entropy [39].

### 3.5 Adsorption Isotherm

The adsorption route is usually regarded as a substitution process between the inhibitor in the aqueous solution [40]. In order to obtain isotherm, the linear relation between surface coverage ( $\theta$ ) value and  $C_{inh}$  must be found. By far the best fit is obtained with the modified Langmuir adsorption isotherm. The following Equation (8) can be used:

$$\theta / (1 - \theta) = K_{ads} C \quad (8)$$

where  $K_{ads}$  is the equilibrium constant of the inhibitor adsorption process and  $C$  is the inhibitor concentration, and  $\theta$  is the degree of the surface coverage, which is calculated using Equation (9):

$$\theta = IE\% / 100 \quad (9)$$

where  $IE\%$  is percentage inhibition efficiency as calculated using Equation (3).

This model has also been used for other inhibitor systems. The plot of  $C_{inh}/\theta$  versus  $C_{inh}$  gives a straight line with intercept  $1/K$  as shown in Figure 7. The slopes of the isotherms show deviation from the value of unity as would be expected for the ideal Langmuir adsorption isotherm equation. This deviation from unity may be due to the interaction among the adsorbed species on the metal surface. The Langmuir isotherm equation is based on the assumption that adsorbed molecules do not interact with one another, but this is not true in the case of organic molecules having polar atoms or groups which are adsorbed on the cathodic and anodic sites of the metal surface. Such adsorbed species may interact by mutual repulsion or attraction. It is safely recommended to not determine  $\Delta G_{ads}$  values since the mechanism of adsorption remains unknown [ ].

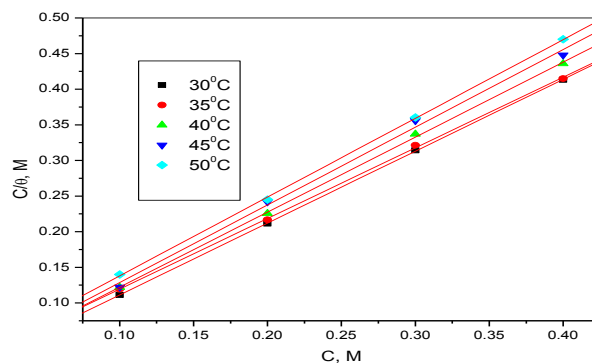


**Figure 7:** Langmuir adsorption isotherms for the adsorption of CPSE on Al in  $H_2SO_4$  (pH =2.3)

### 3.6. Scanning Electron Microscopy and Energy-dispersive X-ray spectroscopy (EDX) analy

The surface morphology of the commercial sample of aluminium was examined by SEM immediately after the sample is subjected to corrosion in H<sub>2</sub>SO<sub>4</sub> medium of pH 2.3 in the absence and in the presence of inhibitor. The SEM image of corroded commercial sample of aluminium is shown in Figure 9(a). It shows degradation of sample. Figure 9(b) represents SEM image of the corroded sample after the in the same medium after the addition of CPSE. The image clearly shows the adsorbed layer of inhibitor molecules on the metal surface thus protecting the metal from corrosion. Results of EDX images are shown in Figure 10(a) and 10(b). From Figure 10(b) it is clear that there is a peak corresponding to nitrogen indicates the adsorption of the inhibitor molecule on the surface of the metal. The results are tabulated in Table 5.

**Table 4:** EDX analysis result of aluminium in H<sub>2</sub>SO<sub>4</sub> (pH=2.3) in the presence and absence of CPSE

Medium	Composition(%)				
	Al	O	Si	S	N
Aluminium in H <sub>2</sub> SO <sub>4</sub>	92.78	7.16	0.37	0.16	-
Aluminium in H <sub>2</sub> SO <sub>4</sub> CPSE + H <sub>2</sub> SO <sub>4</sub>	79.02	7.16	0.38	0.06	0.28

### 3.7. Mechanism of Inhibition

CPSE is composed of numerous naturally organic heterocyclic compounds. Major active constituent is reported [19] to be Benzylisothiocyanate the structure of same is given in Figure 11.

Surface of aluminium is covered with thin layer of  $\gamma$  alumina which initially thickens on exposure to neutral aqueous solution with the formation of a layer of crystalline hydrated alumina. The aluminium surface has positive charge in acidic environment in contact with sulphuric acid [41]. Corrosion of aluminium in acid medium proceeds with following steps:[41].

At anodic area:



The cathodic hydrogen evolution is according to the following steps



CPSE molecule contains nitrogen and sulphur atoms which are rich source of electrons. These atoms from coordinate bond with positively charged metal sites at anodic area and brings anodic process under control. In acidic medium, the inhibitor molecule may get protonated and blocks the cathodic site, there by controlling the cathode reaction.

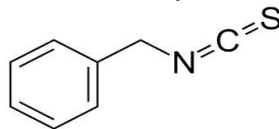


**Figure 11:** Structure of Benzylisothiocyanate.

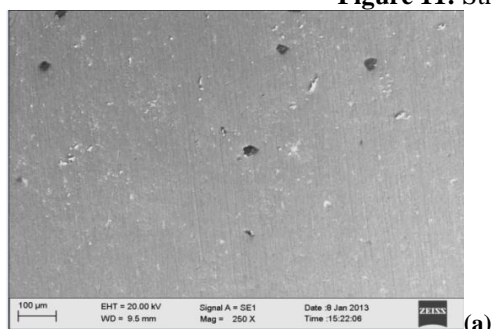


**Figure 9 (a):** SEM image for Al metal in H<sub>2</sub>SO<sub>4</sub>( pH=2.3)



**Figure 9(b):** SEM image for Al metal in H<sub>2</sub>SO<sub>4</sub>( pH= 2.3)+CPSE

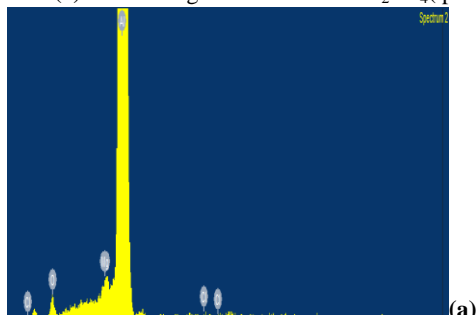


**Figure 10 (a):** EDX spectrum of Al metal in H<sub>2</sub>SO<sub>4</sub> ( pH= 2.3)

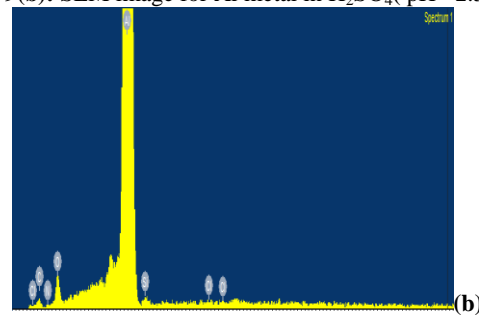


**Figure 10(b):** EDX spectrum of Al metal in H<sub>2</sub>SO<sub>4</sub> ( pH= 2.3) + CPSE

## Conclusion

- CPSE is a cost effective, readily available green inhibitor, for the corrosion control of uminium.
- The inhibition efficiency increases with increase in concentration of CPSE and decreases with increase in temperature.
- CPSE acts as mixed inhibitor, and undergoes physisorption during the inhibition process.

## References

1. Montccoli C, Brunoro G., Frigani A., Zucchi F., *Corros. Sci.* 32 (1991) 693.
2. Moffat T.p., Stafford G.R, and Hall D.E., *J.Electrochem.Soc.* 140 (1993) 2779.
3. Brett C.M.A., Gomes I.A. and Martins J.P.S., *J.Appl.Electrochem.* 24 (1994) 1158.
4. Cabot P.L.,Centellas F.A.Gardo J.A., Perez E.,Vidal H., *Electrochem. Acta.* 36 (1991) 179.
5. Hefter G.T., N.A.North, S.H.Tan., *J. Corros. sci.* 53 (1997) 657.
6. Schmitt G., J.Br., *Corros.* 19 (1984) 1937.
7. Hadi Z.M. Al-Sawaad, Alaa S.K. Al-Mubarak, Athir M. HaddadI., *J. Mater. Environ. Sci.* 1 (4) (2010) 227-238.
8. El Ouali I., Hammouti B., Aouniti A. et al., *J. of Mater. and Environ. Sci.* 1(1) (2010) 1–8.
9. Jamal Abdul Nasser A., Anwar Sathiq M., *Int.J. of Eng. Sci. and Tech* 11 ( 2010) 6417-6426.
10. Etre A.Y.El., *J.Applied Surface science* ., 252(24),(2006), 8521-8525.
11. Hari Kumar and S. Karthikeyan., *J. of Mater. Environ. Sci.* 3 (5) (2012) 925–934.
12. Saratha R., Priya S.V., Thilagavathy P., *J. Chemistry.* 6(3) (2009) 785-795.
13. Raja P.B., Sethuraman M.G., *J.Surface Review and Letters.* 14(6) (2007) 1157-1164.
14. Amitha Rani B.E., Bharathi Bai Basu J., *J.Zastiya Masterijala*, 52 (2011) broj 1.
15. Sangeetha M.1, Rajendran S.1, Muthumegala S.1, Krishnaveni A. 2, *J. Zaštita Materijala*., 52 (2011) broj 1.
16. Deepa Prabhu., Rao Padmalatha., *J. Mater. Environ. Sci.* 4(5) (2013) 732-743.
17. Prabhu D., Rao P., *J. Environ. Chem. Eng.* (2013). (In Press)
18. Deepa, P., Padmalatha, *Arabian Journal of Chemistry* (2013). (In Press)
19. Aravind. G, Debjit Bhawmik 1, Duraivel. S1, Harish. G1, *J. of Medi. Pla. Stu* 1(1) (2013) 7-15.
20. Fabrizio Zucchi, Ibrahim Hashi Omar., *J.Surface technology.* 24 (1985) ,391-399.
21. Adeneye A.A., Olagunju J.A., Banjo A.A.F., Abdul S.F, Sanusi O.A., Sanni O.O., Osarodion B.A., Shonoiki O.E, *Int J App Res Nat prod*, 2 (2009) 19-32.
22. Fontana MG (1987) Corrosion Engineering, 3rd edn. McGraw-Hill, Singapore.
23. Li WH, He Q., Pei CL., Hou BR., *Electrochim Acta.* 52 (2007) 6386.
24. Ferreira ES., Giancomelli C., Giacomelli FC., *Spinelli A Mater Chem Phys* 83 (2004) 129.
25. Li WH, He Q., Pei CL., Hou BR., *J Appl Electro.Chem.* 38 (2008) 289.
26. Amin M A., Abd El-Rehim S S., El-Sherbini E E F., Bayyomi R S J., *Electrochim Acta* 52 (2007) 3588.
27. Brett C.M.A., *J. Appl. Electrochem.* 20 (1990) 1000.
28. Mansfeld F., Lin S., Kim K., Shih H., *Corros. Sci.* 27 (1987) 997.
29. Mansfeld F., Lin S., Kim S., Shih H., *Mater. Corros.* 39 (1988) 487.
30. Brett C.M.A., *Corros. Sci.* 33 (1992) 203.
31. Wit J.H., Lenderink H.J.W., *Electrochim. Acta.* 41 (1996) 1111.
32. Bessone J.B., Salinas D.R., Mayer C., M. Ebert, W.J. Lorenz, *Electrochim. Acta* 37 (1992) 2283.
33. Frers, S.E.; Stefenel, M.M.; Mayer, C.; Chierchie, T., *J. Appl. Electrochem.*, 20(6) (1990) 996–999.
34. Schorr M, Yahalom., *J. Corros. Sci.* 12 (1972) 867.
35. Bouklah M, Hammouti B, Aounti A, Benhadda T., *Prog Org Coat* . 49 (2004) 227.
36. Mansfeld F., Marcel Dekkar, New York, (1987) 119.
37. Sahin M., Bilgic S., Yilmaz H., *Appl. Surf. Sci.* 195 (2002) 1.
38. Ateya B., El-Anadouli., B.E., El-Nizamy F.M., *Corros. Sci.* 24 (1984) 509.
39. Mansfeld F., Tsai C.H., Shih H.: Munn R.S. (Ed.), *ASTM, Philadelphia, PA*, (1992) 86.
40. Oguzie EE, Njoku VO, Enenebeaku CK, Akalezi CO, Obi C., *J. Corros Sci* 50 (2008) 3481.
41. Md. Nazrul Islam Bhuiyan, Jaripa Begum, Mahbuba Sultana, *Bangladesh J Pharmacol*, 4 (2009) 150.

(2014); <http://www.jmaterenvirosci.com>